Article

Not peer-reviewed version

Prolonged Supplementation of Ozonated Sunflower Oil Bestows an Antiaging Effect, Improves Blood Lipid Profile and Spinal Deformities, and Protects Vital Organs of Zebrafish (*Danio rerio*) against Age-Related Degeneration: Two-Years Consumption Study

Kyung-Hyun Cho *, Ashutosh Bahuguna, Dae-Jin Kang, Ji-Eun Kim

Posted Date: 27 November 2023

doi: 10.20944/preprints202311.1671.v1

Keywords: antioxidant; dyslipidemia; kidney; liver; ovary; radio imaging; senescence; testis; zebrafish

Article

Prolonged Supplementation of Ozonated Sunflower Oil Bestows An Antiaging Effect, Improves Blood Lipid Profile and Spinal Deformities, and Protects Vital Organs of Zebrafish (*Danio rerio*) against Age-Related Degeneration: Two-Years Consumption Study

Kyung-Hyun Cho *, Ashutosh Bahuguna, Dae-Jin Kang and Ji-Eun Kim

Raydel Research Institute, Medical Innovation Complex, Daegu 41061, Republic of Korea

* Correspondence: chok@raydel.co.kr; Tel.: +82-53-964-1990; Fax: +82-53-965-1992

Abstract: Ozonated sunflower oil (OSO) is renowned for its diverse therapeutic benefits. Nonetheless, the consequences of extended dietary intake of OSO have yet to be thoroughly investigated. Herein, the effect of 2-year dietary supplementation of OSO was examined on the zebrafish survivability, obesity, skeletal deformities, swimming behavior, and liver, kidney, ovary, and testis function. Results showed that the zebrafish feed supplemented with 20% (*wt*/*wt*) OSO for 2 years emerged with higher survivability and body weight management compared to sunflower oil (SO) and normal diet (ND) supplemented zebrafish. Radio imaging (X-ray) based analysis revealed 2.6° and 15.2° lower spinal curvature in the OSO-supplemented groups than in SO and ND-supplemented groups; consistently, OSO-supplemented zebrafish showed better swimming behavior. The histology analysis of the liver revealed a least fatty liver change and interleukin 6 (IL-6) generation in the OSO-supplemented group. Additionally, a significantly lower level of reactive oxygen species (ROS), apoptotic, and senescent cells were observed in the liver of the OSO-supplemented zebrafish. Also, no adverse effect on the kidney, testis, and ovary morphology was detected during 2 years of OSO consumption. Moreover, lower senescence with diminished ROS and apoptosis was noticed in the kidney and ovary in response to OSO consumption. The OSO supplementation was found to be effective in countering age-associated dyslipidemia by alleviating total cholesterol (TC), triglycerides (TG), low-density lipoproteins (LDL-C) and elevating high-density lipoproteins (HDL-C)/TC levels. Conclusively, prolonged OSO consumption showed no adverse effect on the morphology and functionality of vital organs; in fact, OSO supplementation displayed a protective effect against age-associated detrimental effects on spinal deformities, vital organ functionality, cell senescence, and survivability of zebrafish.

Keywords: antioxidant**;** dyslipidemia; kidney; liver; ovary; radio imaging; senescence; testis; zebrafish

1. Introduction

Sunflower oil (SO) extracted from sunflower seeds is among the major oils used for culinary purposes and has a substantial nutritional and health effect. Linolenic acid and oleic acids are the two primary unsaturated fatty acids that account for 90% of SO's total higher fatty acid content [1]. Additionally, palmitic acid and steric acid have a substantial aggregate and make a significant chunk of unsaturated fatty acids of SO [1,2]. Besides fatty acids, SO is a valuable resource of dietary vitamin E (50-150 mg/100g), primarily α-tocopherol (90%) [3], and minerals like manganese [4]. Though the phytoconstituent of SO is the inherited behavior of the seeds used to extract the SO, it can change substantially with a variety of sunflowers and environmental factors [2]. Many efforts have been

 doi:10.20944/preprints202311.1671.v1

made to improve the constituents of sunflower seeds to enhance the nutritional value and bifunctionality of SO [1]. Mostly, these efforts are focused on the genetic level to obtain sunflower seeds with the desired quality [1]. However, limited efforts have been made on the post-harvest modification of SO. In one such attempt, the thyme and rosemary essential oil was mixed in SO, to maintain the lipid quality of SO compared to the native SO [5].

Ozonation is an additional way that substantially affects the bio-functionality of SO. In ozonation, ozone is pumped into oil where ozone reacts with unsaturated fatty acids via electrophilic addition, leading to the formation of several products such as hydroperoxides and criegee ozonide that impart diverse bio-functionality to the oil [6]. Notably, during ozonation, only unsaturated sites are affected without any impact on the oil's saturated fatty acids and other phytonutrients [7]. Various vegetable oils have been successfully used to develop stable ozonated oils that have been extensively used for antimicrobial agents for topical application [8].

Among the different ozonated oils, SO has been greatly acknowledged for its antimicrobial [9], anti-inflammatory, antioxidant [9,10], and wound-healing role [11,12]. As an antioxidant, ozonated SO (OSO) proved efficient in upregulating cellular antioxidants (SOD) and reduced thiobarbituric acid reactive substances (TBARS) in the gastric mucosa of rats [13]. Also, the role of OSO in enhancing glutathione peroxidase (GSH-PX) and, consequently, its impact on glutathione (GSH) metabolism has been reported [13]. In one of the recent studies, we interpreted the positive impact of OSO on the structural modification of high-density lipoprotein 3 (HDL_3) and HDL_3-associated antioxidant enzyme paraoxonase (PON-1) [9]. Furthermore, the effective contribution of OSO in averting hyperlipidemia induced by a high-cholesterol diet [10], along with as a modulator of inflammation and influence on fibroblast proliferation, collagen fiber remodeling, and tissue regenerative activity, has been noted [13]. Numerous studies have elucidated the crucial therapeutic benefits of OSO in combating various ailments [14-17]; nevertheless, investigations on the prolonged dietary intake of OSO and its associated health consequences have yet to be initiated. Therefore, this research was initiated to assess the impact of sustained long-term consumption of OSO on the health of zebrafish, aiming to explore the potential of OSO as a functional food.

Considering this into account, the present study was performed to examine the impact of OSO supplementation in the diet for 2 years on the survivability, body weight, structural deformities, swimming behavior, lipid profile, and functionality of the zebrafish's vital organs (liver, kidney, testis, and ovary). Furthermore, an assessment of the effect of OSO on age-related cellular senescence was conducted.

2. Materials and Methods

2.1. Materials

The ozonated sunflower oil (Raydel®, Bodyone, Flambo oil) with a characteristic Oleozone® [18] was obtained from Rainbow and Nature Pty, Ltd. (Thornleigh, NSW, Australia). The sunflower oil (Ondoliva oil, Urzante, Spain) was procured from a local supermarket in Daegu, Republic of Korea. Acridine orange (Cat#A9231), dihydroethidium (Cat#37291), 2 phenoxyethanol (Cat#P1126), 5-bromo-4-chloro-3-indolyl β D-galactopyranoside (X-gal, B4252), and oil red O (Cat#O0625) were purchased from Sigma-Aldrich (St. Louis, MO, USA). Unless specified, all remaining reagents were of high purity and utilized as provided.

2.2. Preparation of Sunflower Oil (SO) and Ozonated Sunflower oil (OSO) Supplemented diet

The normal tetrabit (Tetrabit Gmhb D49304, Melle, Germany), a regular zebrafish food, was blended with 20% SO (*wt/wt*) or 20% OSO (*wt/wt*). The SO and OSO-supplemented normal tetrabit was agitated vigorously to obtain the homogeneous distribution of SO and OSO.

2.3. Zebrafish Aquaculture

Zebrafish were upheld in a water tank sustained at 28°C temperature with constant automated aeration (Bioengineering Company, Daejeon, Republic of Korea) following the prescribed rules of

care and use of laboratory animals [19,20] adopted by the Animal Care Committee and the Use of Raydel Research Institute (approval code RRI-20-003). A light (14 hr) and dark (10 hr) photoperiod was maintained during the zebrafish husbandry. Zebrafish were fed with normal tetrabit.

2.4. Zebrafish Fed with Sunflower Oil (SO) and Ozonated Sunflower Oil (OSO)

The 8-week-aged zebrafish (n=240) underwent random allocation to three cohorts (n=80, each group). Zebrafish in group I received normal tetrabit (ND and considered as control), while the zebrafish in group II were maintained in ND supplemented with 20% SO (*wt/wt*). Likewise, the zebrafish in group III were maintained in ND supplemented with a 20% OSO (*wt/wt*) diet. All the groups were maintained under similar environmental conditions. Zebrafish survivability in each group was recorded at different time points (0 to 24 months). Correspondingly, the zebrafish's weight across all three groups was reported (from 0 to 24 months) after anesthetization of the zebrafish by immersing them in a 0.1% solution of 2-phenoxyethanol.

2.5. Radiology Imaging

Zebrafish (28 months old) from the different groups were anesthetized by submerging them into a 0.1% solution of 2-phenoxyethanol. The anesthetized zebrafish were processed for whole skeleton radiology imaging using an X-ray machine (Woorien, Myvet dent model, Hwaseong, Korea) at an accelerating voltage of 50 and f stop of 15 sec (Siji W Animal Medical Center, Daegu, Korea). The obtained image was processed by Intovet, into CNS imaging software. For the quantification of the spinal bending, an angle was determined through Image J software (http://rsb.info.nih.gov/ij/, 1.53 version assessed on 2023 Jan 30). The angle of spinal bending was calculated between vertebra 1 and 24, considering vertebra 5 a central point.

2.6. Histology and Immunohistochemical Analysis

At 24 months, zebrafish (n=10) from different groups were sacrificed using the hypothermic shock [10], and different organs (liver, kidney, ovary, and testis) were surgically removed and preserved in 10% formalin. The tissue from the different organs was individually dehydrated using ethanol and subsequently embedded into paraffin wax, followed by tissue sectioning (7 μm thick). Liver, kidney, ovary, and testis tissue sections underwent processing for Hematoxylin and Eosin (H&E) staining [21] to assess morphological changes.

The tissue section from the liver was also processed for the fatty liver changes using oil red O staining, following the method described previously [22]. Briefly, oil red O stain (final, 3 mg/mL) was spread over the tissue section. After 10 min incubation, the stained area was washed with tap water and observed under the microscope (Motic SMZ 168; Hong Kong).

Immunohistochemical (IHC) staining was employed for interleukin 6 (IL-6) production in hepatic tissue as a previously described method [23]. The hepatic tissue section (7 μm thick) was immersed with IL-6 specific primary antibody and incubated at 4°C for 18 hr. After that, the tissue section was developed by using HRP conjugated anti-IL-6 antibody using EnVison + System HRP labeled polymer kit (Code K4001, Dako, Glostrup, Denmark) and observed under a microscope (Motic SMZ 168; Hong Kong). To enhance the clarity of presentation, the IL-6-stained area (originally brown) was replaced with a red color when the brown color threshold value was set between 20 and 120 using Image j software (http://rsb.info.nih.gov/ij/, version 1.53, appraised on 2023 January 30).

2.7. Imaging for Reactive Oxygen Species (ROS) and Apoptosis

The method described earlier [24] was employed to assess the production of reactive oxygen species (ROS) in the tissue section using dihydroethidium (DHE) fluorescent staining. Briefly, a 250 μL of DHE solution (final, 30 μM) was added to the tissue section. Following 30 min incubation in the dark, the stained area was rinsed with tap water and observed using a fluorescent microscope (Nikon Eclipse TE2000, Tokyo, Japan) with excitation at 588 nm and emission at 605 nm wavelength. The extent of apoptosis was examined using acridine orange (AO) fluorescent staining, following a

 doi:10.20944/preprints202311.1671.v1

method described previously [25]. In summary, a tissue section was treated with 250 µL of AO (5 µg/mL) and visualized under a fluorescent microscope (Nikon Eclipse TE2000, Tokyo, Japan) at an excitation wavelength of 502 nm and an emission wavelength of 525 nm.

2.8. Senescence-Tied β Galactosidase Staining

A previously described senescence-associated β galactosidase (SA-β-gal) staining method [26] with slight modification was implemented to examine the senescent cells in the liver, kidney, testis, and ovary. Briefly, a tissue section (7 µm thick) underwent fixation using 4% paraformaldehyde and incubated for 5 minutes at room temperature (RT), followed by two washes with phosphate-buffered saline (PBS). The tissue section was flooded with X-gal solution [X-gal (final, 1 mg/mL) dissolved in citrate-phosphate buffer (pH 5.9) containing 5 mM each of ferric and ferro cyanide, 150 mM NaCl, 2 mM of $MgCl_2$)] and incubated in the dark for 16 hr, following two times washing with PBS and visualization under the microscope (Motic SMZ 168; Hong Kong).

2.9. Analysis of Blood Lipid profile and Biomarkers Associated with Liver Function

A 2 µL of blood was collected from the zebrafish's heart and instantly mixed with 5 µL of PBS-ethylenediaminetetraacetic acid (EDTA, final 1 mM). The collected plasma proceeded for the quantification of total cholesterol (TC), triglycerides (TG), and high-density lipoproteins (HDL-C) using the commercial diagnostic kit (cholesterol, T-CHO, and TGs, Cleantech TS-S; Walko Pure Chemical, Osaka, Japan). The low-density lipoproteins (LDL-C) concentration in the blood plasm was calculated using the Friedewald equation: [TC–HDL–(TG/5)].

The commercial diagnostic kit (Asan Pharmaceutical, Hwasung, Republic of Korea) was used to quantify aspartate transaminase (AST) and alanine transaminase (ALT) levels in the serum, following the instructions suggested by the manufacturers.

2.10. Statistical Analysis

The results are depicted as the mean ± standard deviation from three distinct experiments. Statistical analysis was conducted using the Statistical Package for the Social Science (SPSS version 29.0; Chicago, IL, USA), employing one-way analysis of variance (ANOVA) followed by Tukey's multiple range test to identify significant distinctions among the groups.

3. Results

3.1. Zebrafish Survivability and Body Weight

The survivability of zebrafish in all the groups progressively decreases with the progression of time (Figure 1 A). At the end of 12 months, supplementation of SO and OSO groups showed a nearly similar survivability of 96.3% and 95.4%, respectively, which is slightly better than the survivability observed in the ND group (92.5%). However, at the end of 17 months, the least survivability (87.5%) was observed in the SO group, followed by the ND group (90.0%). In contrast, the OSO feed group showed much higher survivability (93.9%). Consistent with 17 months, no changes in the zebrafish survivability were observed at 18 months of feeding in ND and OSO groups; unlike this, survivability decreased and reached 85.0% in the SO group. Interestingly, at 21 months onwards, OSO-supplemented groups displayed nearly constant survivability. Contrary to this, the ND and SO-supplemented groups revealed a sharp decline in survivability during 21 months to 24 months of feeding. At the final 24 months, 81.8%, 72.5%, and 71.2% survivability were observed in OSO, SO, and ND groups, i.e., 18.2%, 27.5%, and 28.8% lower than the survivability observed at the initial day. Results clearly demonstrated that OSO substantially affects zebrafish survivability, i.e., 9.3% and 10.6% better than the zebrafish survivability observed in SO and ND groups after 24 months of feeding.

A time-dependent change in the body weight of zebrafish was recorded up to 24 months, and results are depicted in Figures 1 B and C. After 12 months, consumption of SO-supplemented group

Preprints (www.preprints.org) | NOT PEER-REVIEWED | Posted: 27 November 2023 doi:10.20944/preprints202311.1671.v1

body weight (520.2±20.7 mg) increased by 72.2% than its initial day value (301 mg±10.9 mg). Contrary to this, 30.39% and 29.3% changes in body weight were observed after 12 months in OSO (392.5±15.8 mg) and ND (389.4±12.8 mg) fed groups conversely their initial day weight. The maximum bodyweight (885.7±57.5 mg) was detected in the OS-fed group, i.e., 2.0-fold (439.1±20.2 mg) and 1.6-fold (540.8±29.8 mg) fold higher than the bodyweight of OSO and ND-fed groups at 18 months. From 18 months onwards, the body weight of OSO and ND-supplemented groups remained almost constant. Contrary to this, a sharp decline in body weight was perceived in the SO-supplemented group at 24 months than at 18 months. At 24 months, a significantly 1.3-fold (p<0.025) and 1.2-fold (p<0.018) higher body weight was noticed in the SO-supplemented group than in the body weight of OSO and ND-supplemented groups. The results suggest that OSO supplementation had no adverse effect on the enhancement of body weight, unlike SO supplementation, which severely impacts body weight enhancement.

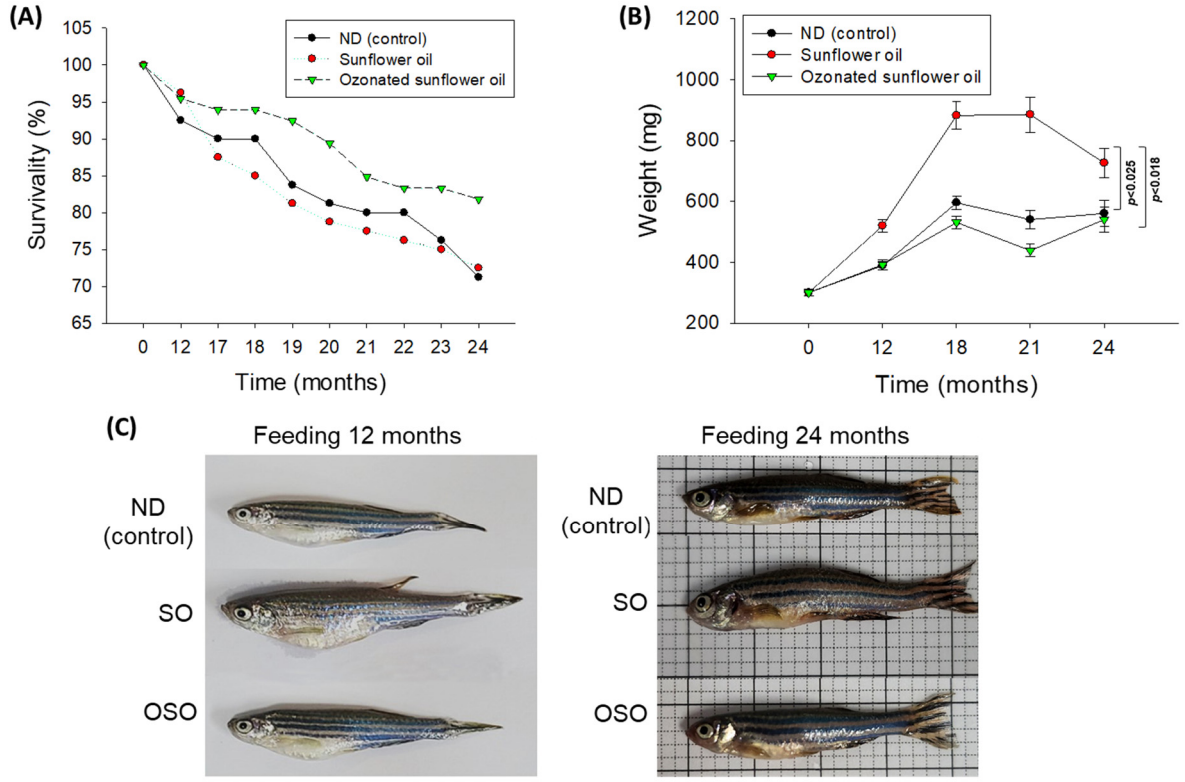

Figure 1. Long-term supplementation of sunflower oil (SO) and ozonated sunflower oil (OSO) on survivability and body weight of zebrafish. **(A)** Time-dependent survivability. **(B)** A time-dependent change in body weight. **(C)** Morphological changes at 12 and 24 months feeding. ND represents the control normal diet; SO represents ND supplemented with 20% SO (*wt*/*wt*); OSO represents ND supplemented with 20% OSO (*wt*/*wt*).

3.2. Radiology Imaging for the Structural Deformities and Swimming Behavior of Zebrafish

Age-associated structural (backbone) bending was determined at 28 months post-feeding in ND, SO, and OSO-supplemented groups, and results were compared with ND feed 14 months young zebrafish. The visual examination revealed no backbone structural deformities in ND and OSO-supplemented (Figure 2 A). Unlike this, severe backbone bending was observed in the SO-supplemented group (Figure 2 A). Further bending of the zebrafish backbone in different groups was quantified by radio imaging of the spine (Figure 2 B-D). Radio imaging revealed a 164.1±2.1° spinal angle in the ND feed 14 months aged zebrafish, which is used as a reference to evaluate the alteration in the spinal bending in ND, SO, and OSO-supplemented groups. In the ND-supplemented group, a 152.1±2.8° of spinal bending was observed, i.e., significantly 7.2% (p<0.005) altered than the reference spinal bending of 14 months aged zebrafish. Contrary to the ND group, the OSO group showed non-

Preprints (www.preprints.org) | NOT PEER-REVIEWED | Posted: 27 November 2023 doi:10.20944/preprints202311.1671.v1

significant changes in spinal bending (156.3±1.6°) compared to the reference (14 months aged zebrafish). While compared to ND, the OSO group exhibited 2.6° retardation in spinal bending. The most adverse results were observed in the SO-supplemented group where severe spinal bending was noticed, i.e., significantly 19.1% (p<0.001), 12.2% (p<0.001), and 15.2% (p<0.001) altered than the 14 months aged, ND, and OSO-supplemented groups.

Consistent with the findings of spinal bending, a difference in swimming behavior was observed between the groups (Supplementary video S1). The normal swimming behavior (higher swinging speed) was observed in the OSO-supplemented group, followed by ND-supplemented zebrafish at 28 months post-feeding. In contrast, severe retardation in the swimming activity was observed in the SO feed group.

A collective outcome revealed the impact of prolonged OSO consumption on preventing age-associated spinal deformities, tissue regeneration, and, consequently, their swimming and locomotory behavior.

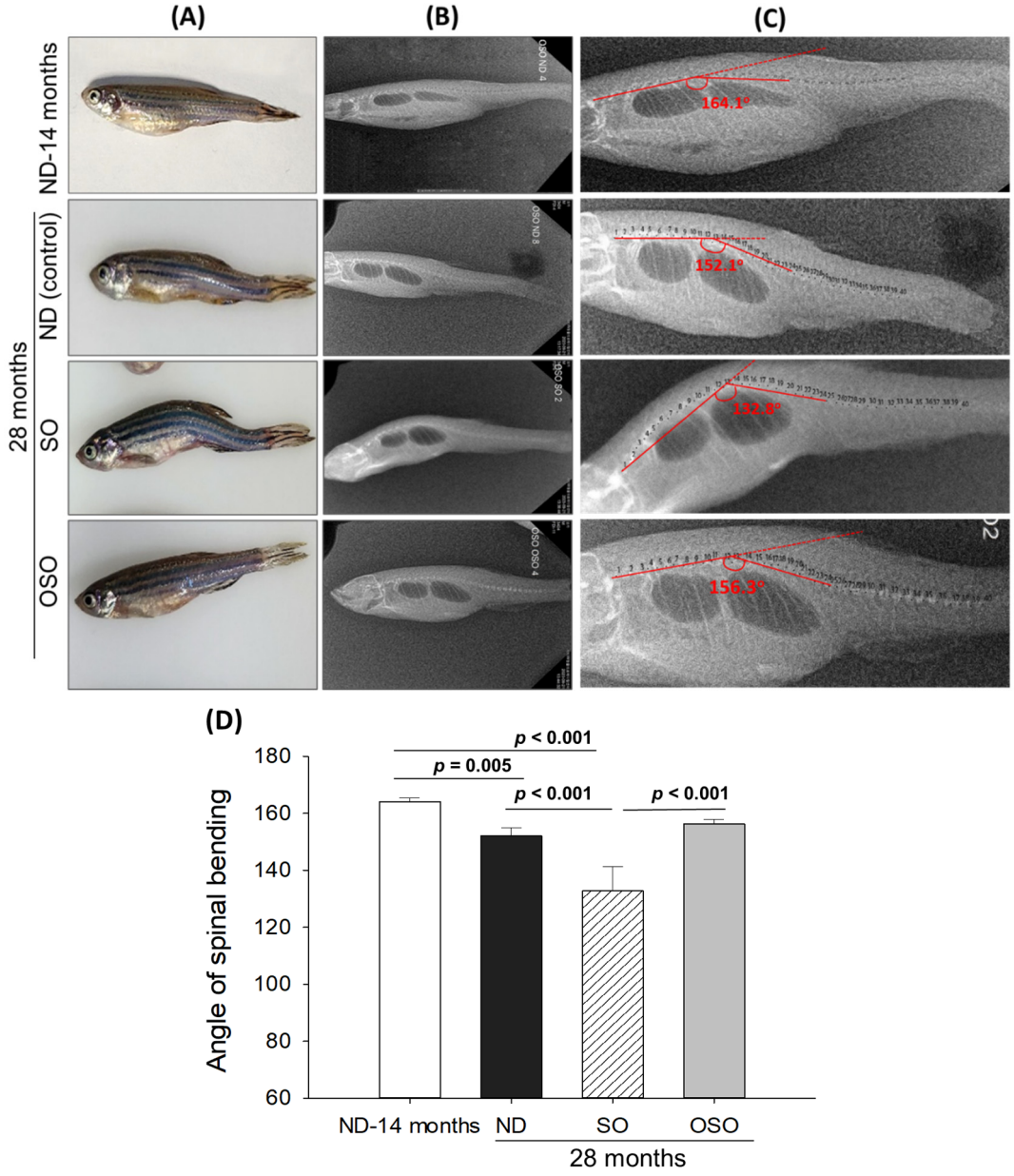

Figure 2. Age-related structural deformities in zebrafish at 28 months supplementation of sunflower oil (SO) and ozonated sunflower oil (OSO). **(A)** A pictorial view representing structural deformities. **(B)** X-ray images and **(C)** and digitally zoomed X-ray images of the zebrafish skeletal (backbone). **(D)** The angle of the spinal deformities (bending) was determined employing image J

 doi:10.20944/preprints202311.1671.v1

software (http://rsb.info.nih.gov/ij/, version 1.53 assessed on 2023 Jan 30). ND represents the control normal diet; SO represents ND supplemented with 20% SO (*wt*/*wt*); OSO represents ND supplemented with 20% OSO (*wt*/*wt*).

3.3. Evaluation of the Liver Section

The H&E staining results, as depicted in Figures 3 A and B, revealed a dilatated portal vein with visible hepatic degeneration in the SO-supplemented group. In contrast, no hepatic degeneration was noticed in the OSO-supplemented groups; however, a minor hepatic degeneration was noticed around the portal vein of the ND-supplemented group. Results also exhibited the presence of neutrophils in the vicinity of the portal vein across the groups. However, the maximum amount was observed in ND, followed by SO and OSO-supplemented groups that account for 21.46%, 18.0%, and 15.9% of the H&E-stained area, respectively. Also, the presence of lipid accumulation (pointed by the yellow arrow) was observed only in the SO-supplemented group, signifying the impact of high amount and prolonged consumption of SO on liver steatosis. The result suggests no adverse effect of OSO supplementation over a long time on hepatic tissue; even more, OSO displayed a positive impact on age-associated adversity, evidenced by a 1.3-fold (p<0.045) reduced H&E-stained area compared to the ND-supplemented group.

Cell senescence is an ideal marker for aging and age-related disorders. The SA-β-gal activity in the hepatic tissue of the ND, SO, and OSO-supplemented groups was evaluated, and results are depicted in Figures 3 A and B. Age-related cell senescence, which was evident by a blue-stained area (denoted by a red arrow), was observed in the ND-supplemented group. In contrast, supplementation of SO for 24 months significantly (p<0.032) elevated hepatocyte senescent. Contrary to this, OSO supplementation displayed a significant 2.3-fold (p<0.041) reduced senescent stained area compared to SO-supplemented groups, signifying the importance of OSO in preventing the liver from age-related adversity.

The ROS level in the hepatic tissue at 24 months of ND, SO, and OSO supplementation was evaluated by DHE fluorescent staining. As depicted in Figures 3 A and B, the highest ROS production was noticed in the SO group, which was significantly 1.6-fold (p<0.001) more than the ROS level detected in the ND group, thus indicating the impact of long-term consumption of SO on hepatic ROS production. The least ROS production was perceived in the OSO-supplemented group, which was significantly 4.1 (p=0.001) and 7.1-fold (p<0.001) lower than the ROS production detected in ND and SO supplement groups, respectively. The results clearly indicated OSO's influential role in protecting the liver from age-induced ROS generation and oxidative stress.

The extent of apoptosis evaluated by AO fluorescent staining revealed the highest apoptosis in the SO-supplemented group (Figure 3 A and B). The ND and OSO-supplemented groups quantified approximately 1.5-fold (p<0.001) reduced apoptosis compared to SO. Notably, no conspicuous variance in hepatic apoptosis was observed between ND and OSO-supplemented groups, which signifies that prolong consumption of OSO did not affect the induction of apoptosis in the liver, asserting it safe to consume.

Preprints (www.preprints.org) | NOT PEER-REVIEWED | Posted: 27 November 2023 doi:10.20944/preprints202311.1671.v1

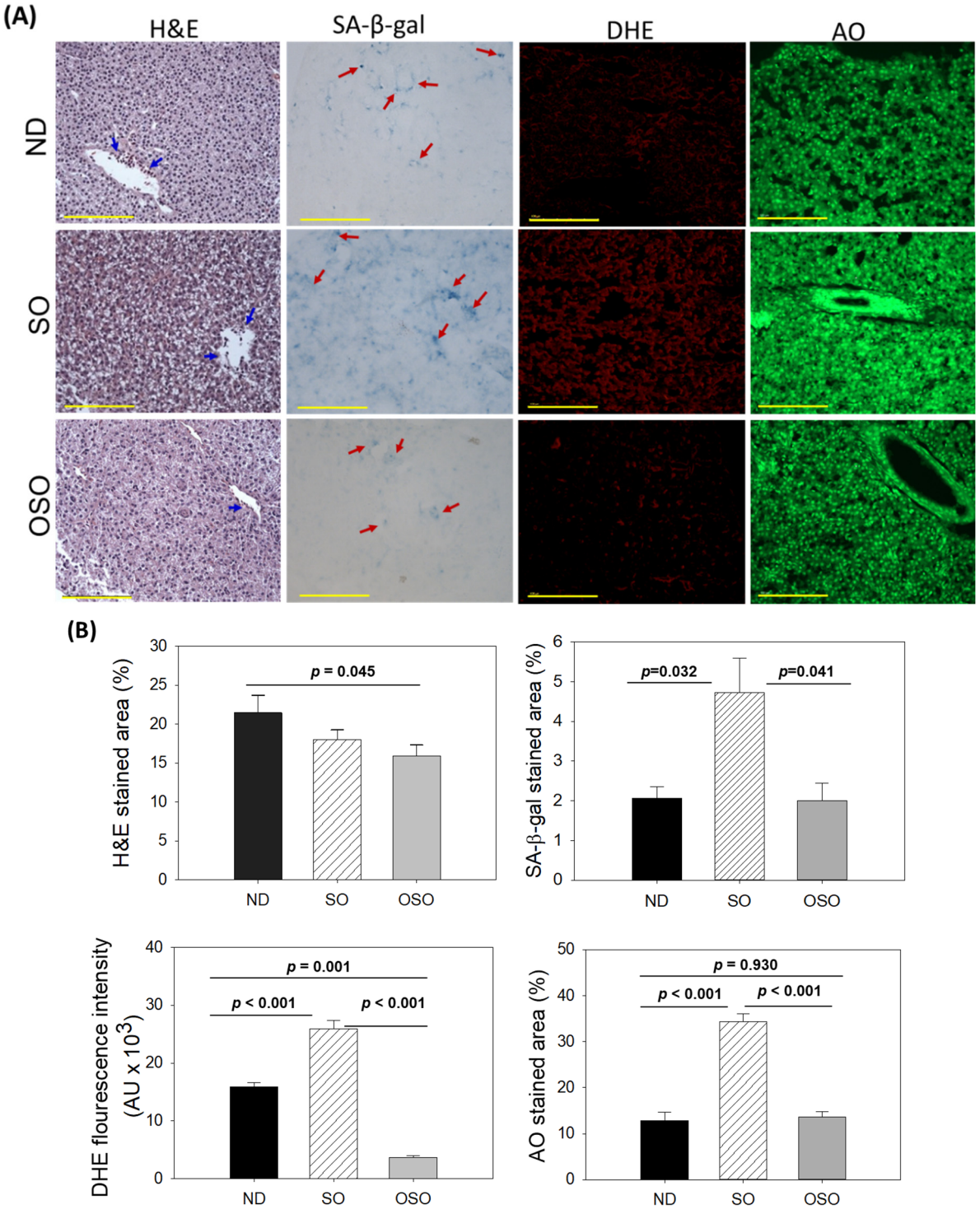

Figure 3. A comparative assessment of 24 months supplementation of sunflower oil (SO) and ozonated sunflower oil (OSO) on the hepatic tissue of zebrafish. **(A)** Hematoxylin and eosin (H&E) staining, senescence-associated β galactosidase (SA-β-gal) staining, dihydroethidium (DHE) and acridine orange (AO) fluorescent staining. [0.1 mm, scale bar]. **(B)** Image j (http://rsb.info.nih.gov/ij/, version 1.53 assessed on 2023 Jan 30) based quantification of H&E and SA-β-gal-stained area, fluorescent intensities of DHE and AO-stained area. ND represents the control normal diet; SO represents ND supplemented with 20% SO (*wt*/*wt*); OSO represents ND supplemented with 20% OSO (*wt*/*wt*). The *p* value signifies the statistical significance discerned between groups resulting from the one-way ANOVA following Tukey's Post Hoc analysis.

Preprints (www.preprints.org) | NOT PEER-REVIEWED | Posted: 27 November 2023 doi:10.20944/preprints202311.1671.v1

3.4. Assessment of Fatty Liver Changes and Inflammation in Liver

As depicted in Figure 4 A and D, a higher oil red O-stained area emerged in the SO supplemented group, suggesting the prolonged consumption of SO-associated with fatty liver changes. Likewise, a substantial oil red O-stained area appeared in the ND group after 24 months of supplementation, exhibiting age-associated fatty liver changes. Notably, a significant 2.7-fold (p<0.001) and 2.5-fold (p<0.001) reduced oil red O-stained area was detected in the OSO-supplemented group compared to the SO and ND-supplemented group, which signifies a constant consumption of OSO to prevent age-related fatty liver changes. Figure 4 (B-E) depicts the IHC stained area representing IL-6 production in hepatic tissue following 24 months of ND, SO, and OSO supplementation. The higher IL-6 level was noticed in the SO-supplemented group, which is significantly 1.2 (p<0.008) and 4.5-fold (p<0.001) higher than the IL-6 production quantified in ND and OSO-supplemented groups, respectively. While compared to ND, OSO logged 3.3-fold (p<0.001) low IL-6 production. The results imply the impact of prolonged consumption of OSO to diminish age-associated IL-6 production in liver.

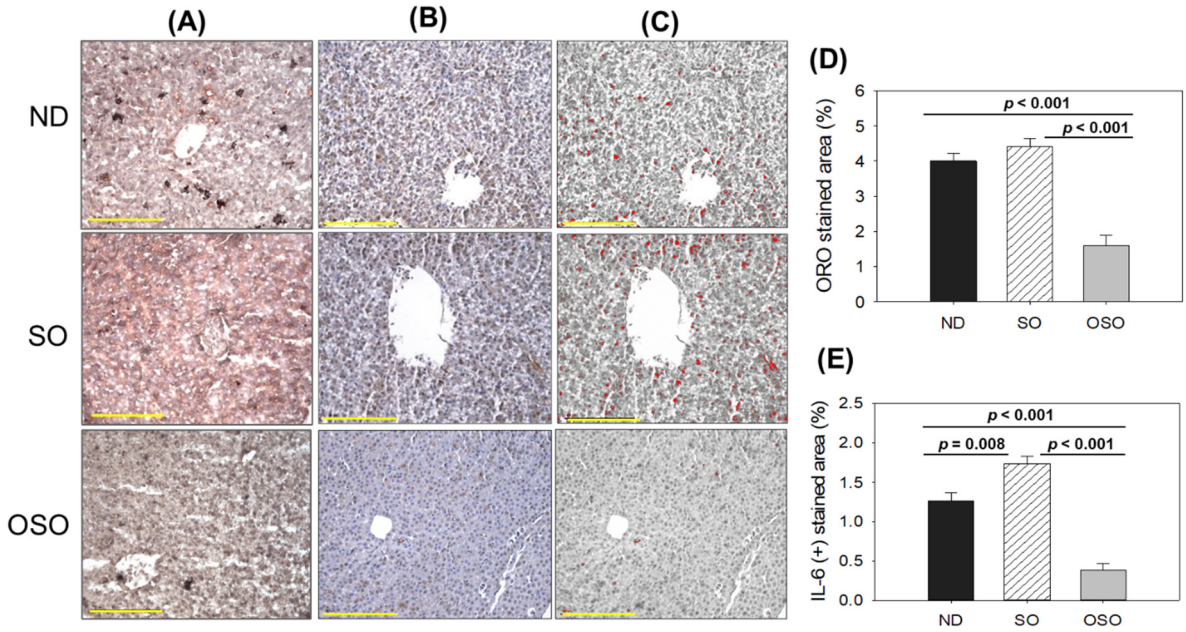

Figure 4. A comparative effect of 24 months supplementation of sunflower oil (SO) and ozonated sunflower oil (OSO) on fatty liver alterations and IL-6 production in zebrafish. **(A)** Oil red O staining. **(B)** Immunohistochemistry (IHC) for the assessment of IL-6 generation. **(C)** Employing Image J software (http://rsb.info.nih.gov/ij/ assessed on 2023 Jan 30), the brown color of the native IL-6-stained area has interchanged with red color, employing a brown color threshold value from 20 to 120.. to intensify the visualization of IHC stained area. **(D)** and **(E)** Quantification oil red O stained and IL-6-stained area employing image J software. ND represents the control normal diet; SO represents ND supplemented with 20% SO (*wt/wt*); OSO represents ND supplemented with 20% OSO (*wt/wt*). The *p* value signifies the statistical significance discerned between groups resulting from the one-way ANOVA following Tukey's Post Hoc analysis.

3.5. Evaluation of Hepatic function Biomarkers

The blood analysis was performed to evaluate important hepatic function biomarkers. As depicted in Figure 5 A, the maximum AST level was spotted in the SO-supplemented group, i.e., 1.2-fold higher than the AST level quantified in the ND group. Contrary to this, the OSO-supplemented group displayed the least amount of AST, i.e., significantly 1.4 (p=0.002) and 1.7-fold (p=0.004) lower than the AST level quantified in ND and SO-supplemented groups, respectively. Like the AST, the utmost ALT level was observed in the SO-supplemented group, i.e., 10.1% and 40.3% higher than the ND and OSO feed group (Figure 5 B). Compared to the ND-supplemented group OSO, supplemented

Preprints (www.preprints.org) | NOT PEER-REVIEWED | Posted: 27 November 2023 doi:10.20944/preprints202311.1671.v1

groups displayed 33.1% lower ALT level. The outcomes align well with the hepatic histology observations, validating OSO's role in safeguarding the liver from age-related deterioration and establishing its non-toxic nature.

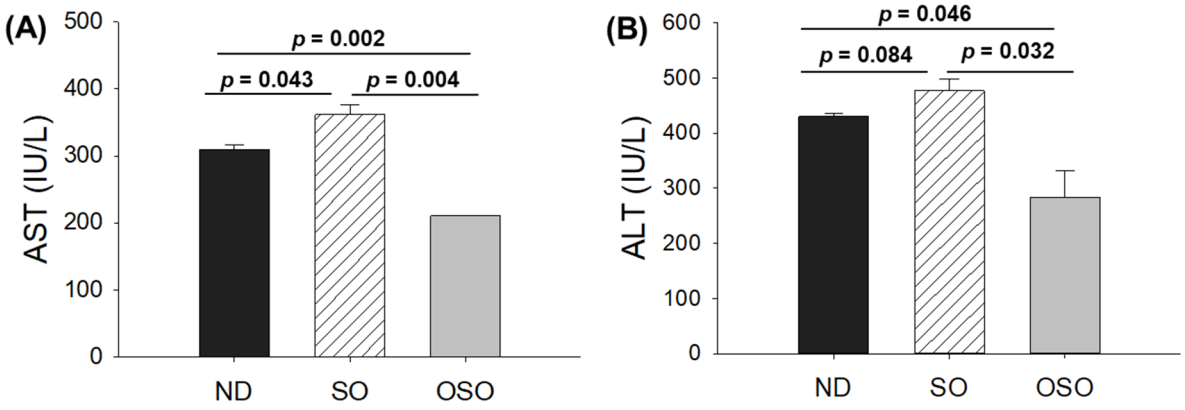

Figure 5. A comparative effect of 24 months supplementation of sunflower oil (SO) and ozonated sunflower oil (OSO) on the hepatic function biomarkers **(A)** Aspartate aminotransferase (AST) and **(B)** Alanine aminotransferase (ALT). ND represents the control normal diet; SO represents ND supplemented with 20% SO (*wt/wt*); OSO represents ND supplemented with 20% OSO (*wt/wt*). The *p* value signifies the statistical significance discerned between groups resulting from the one-way ANOVA following Tukey's Post Hoc analysis.

3.6. Evaluation of the Kidney Section

The results of H&E staining (Figure 6A) revealed a densely packed renal structure with a distinct distal and proximal tubule in the kidney section of ND and OSO-supplemented groups. However, compared to OSO a, luminal cell debris (indicated by the red arrow) was noticed in the tissue section of the ND-supplemented group. In contrast to ND and OSO, a loosely packed and sparsely populated renal tissue structure with certain lumen cell derbies (indicated by a red arrow) was noticed in the tissue section of the SO-supplemented group. However, no sign of severe nephrotoxicity was observed in any groups, evidenced by the absence of proximal convoluted tissue, severe lumen cell debris, and basophilic clusters comprising new nephron formation. Results imply no adverse effect of prolonged OSO supplementation on kidney functionality.

The senescence examined by SA-β-gal activity revealed the highest senescent stained area (indicated by blue arrows) in the SO-supplemented group, followed by ND and OSO-supplemented group, and signifies the provocative role of SO consumption on the age-related senescence in the kidney (Figure 6 B, E). On the contrary, a prolonged supplementation of OSO had an inhibitory effect against age-associated senescence, evidenced by a significantly 2.5-fold (p=0.004) reduced senescence-stained area compared to the ND-supplemented group. Also, OSO supplementation displayed a significantly 2.9-fold (p=0.002) lower senescence-stained area than the SO-supplemented group, signifying the antiaging effect of OSO supplementation.

The DHE fluorescent staining depicted in Figures 6 C and F, revealed the highest ROS production in the SO-supplemented group, followed by the ND-supplemented group. The least ROS production was observed in the OSO-supplemented group, which is significantly 1.3 (p=0.041) and 1.8-fold (p=0.018) lesser than the ROS production noticed in the ND and SO-supplemented groups, signifying the impact of OSO on diminished age-induced ROS production in the kidney.

The AO staining represents the elevated extent of apoptosis in the SO-supplemented group, which is significantly 1.1 (p<0.001) and 1.6-fold (p<0.001) higher than the extent of apoptosis in ND and OSO-supplemented groups, respectively (Figures 6 D, G). While compared to the ND, the OSO supplementation exhibited a noteworthy 1.4-fold reduction in AO fluorescent intensity, testifying to the potential of OSO in mitigating age-induced apoptosis in the kidney.

Preprints (www.preprints.org) | NOT PEER-REVIEWED | Posted: 27 November 2023 doi:10.20944/preprints202311.1671.v1

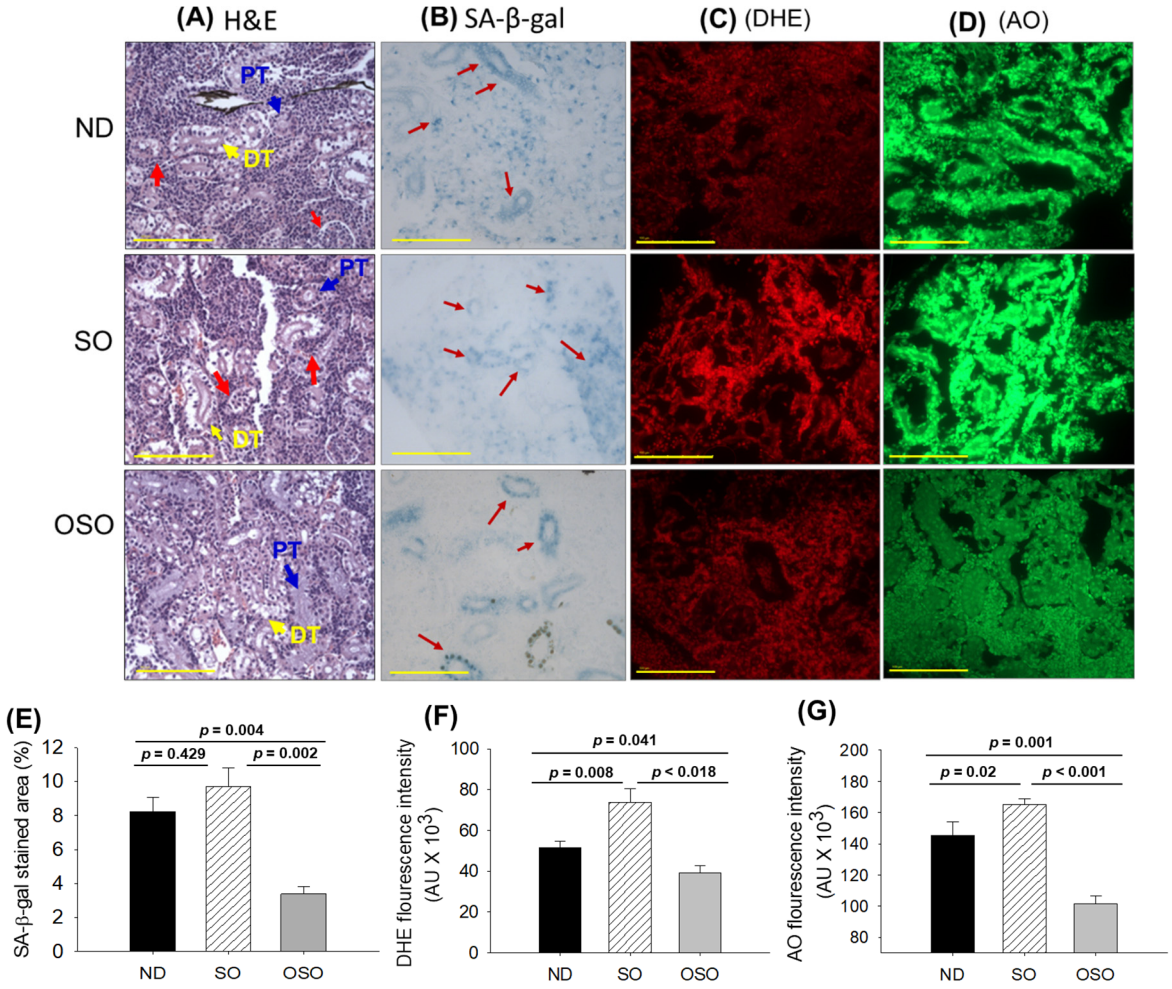

Figure 6. A comparative effect of 24 months supplementation of sunflower oil (SO) and ozonated sunflower oil (OSO) on the kidney of zebrafish. **(A)** Hematoxylin and eosin (H&E) staining. PT and DT symbolize the proximal and distal tubules, respectively. The red arrows indicate luminal debris. **(B)** Senescence-associated β galactosidase (SA-β-gal) staining. Red arrows indicate senescent area. **(C)** Dihydroethidium (DHE) fluorescent staining. **(D)** Acridine orange (AO) fluorescent staining [0.1 mm, scale bar]. Quantification of **(E)** SA-β-gal-stained area, **(F)** DHE and **(G)** AO-stained area utilizing image J software (http://rsb.info.nih.gov/ij/ assessed on 2023 Jan 30). ND represents the control normal diet; SO represents ND supplemented with 20% SO (*wt*/*wt*); OSO represents ND supplemented with 20% OSO (*wt*/*wt*). The *p* value signifies the statistical significance discerned between groups resulting from the one-way ANOVA following Tukey's Post Hoc analysis.

3.7. Evaluation of the Ovary Section

The H&E staining (Figure 7A and B) showed a higher prevalence of previtellogenic in ND and SO-supplemented groups, i.e., significantly 1.7-fold more elevated than the previtellogenic-oocytes that appeared in the OSO-supplemented group. Contrary to this, early vitellogenic oocyte presence is approximately 2.3-fold higher in the OSO-supplemented group compared to ND and OSO-supplemented groups. Likewise, the number of mature vitellogenic is approximately 5-fold higher in OSO-supplemented groups compared to ND and SO-supplemented groups. In addition, degenerated/atretic previtellogenic (indicated by the red arrow) was noticed in the ND and SO-supplemented groups. Results described the prevention of ovary architecture against age-impaired effect in the OSO-supplemented group.

The SA-β-gal staining depicted in Figures 7 A and C revealed the high prevalence of blue-stained senescence area (indicated by the red arrow) in the ovary section of the SO-supplemented group. In comparison to the SO-supplemented group, a significantly 4.3-fold ($p<0.05$) and 6.1-fold ($p<0.037$) lower senescence area was detected in ND and OSO-supplemented groups, respectively. In contrast

Preprints (www.preprints.org) | NOT PEER-REVIEWED | Posted: 27 November 2023 doi:10.20944/preprints202311.1671.v1

to the ND-supplemented group, the OSO-supplemented group exhibited a 1.4-fold reduction in senescence area, indicating that the consumption of OSO does not pose any toxicological implication leading to ovarian senescence. The DHE fluorescent staining revealed a significantly 1.6-fold (p<0.007) and 2.6-fold (p<0.001) higher ROS production in the SO-supplemented group compared to the ND and OSO-supplemented groups (Figure 7 A and D). The zebrafish supplemented with OSO exhibited the lowest production of ROS, which was significantly 1.5-fold (p=0.001) lower than the ND-supplemented group.

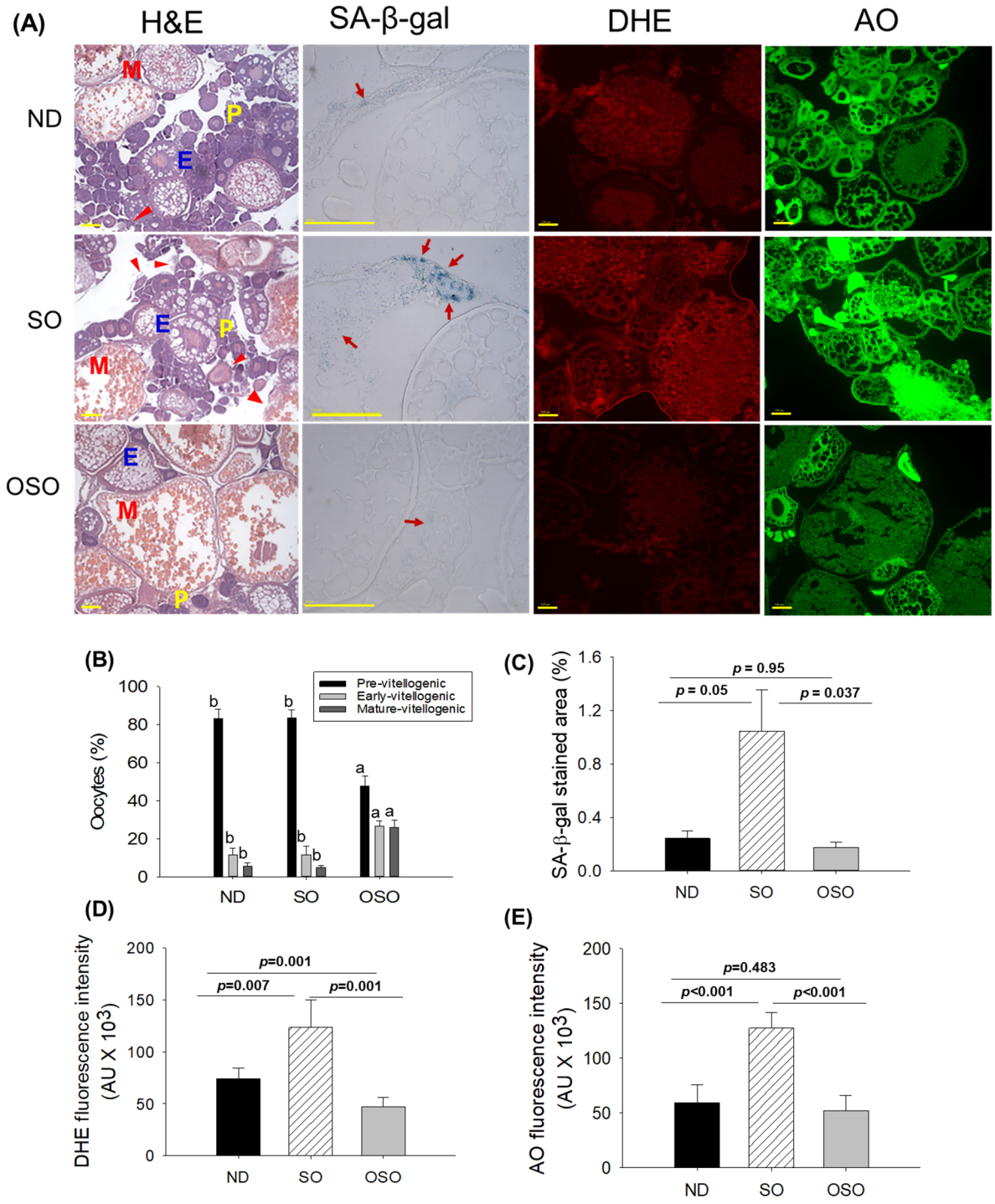

Figure 7. A comparative effect of 24 months supplementation of sunflower oil (SO) and ozonated sunflower oil (OSO) on the ovary of zebrafish. **(A)** Ovarian cell morphology was analyzed by Hematoxylin and eosin (H&E) staining (P, E, and M represents pre, early and mature- vitellogenin stages, respectively), senescence-associated β galactosidase (SA-β-gal) staining (red arrow indicating

 doi:10.20944/preprints202311.1671.v1

senescent area.), dihydroethidium (DHE) and acridine orange (AO) fluorescent staining. [0.1 mm, scale bar]. **(B)** Quantification of the different developmental stages of oocytes based on the H&E images. **(C), (D)** and **(E)** Image J software (http://rsb.info.nih.gov/ij/ assessed on 2023 Jan 30) based quantification of SA-β-gal-stained area, DHE and AO-stained area, respectively. ND represents the control normal diet; SO represents ND supplemented with 20% SO (*wt*/*wt*); OSO represents ND supplemented with 20% OSO (*wt*/*wt*). The alphabets (a,b) above the bar graphs showed the statistical difference between the groups. The *p* value signifies the statistical significance discerned between groups resulting from the one-way ANOVA following Tukey's Post Hoc analysis.

Similar to the DHE staining, an elevated extent of apoptosis was noticed in SO-supplemented groups compared to the ND-supplemented group (Figure 7 A and E). The least apoptosis was evaluated in OSO-supplemented groups, i.e., 1.1-fold and 2.4-fold ($p<0.001$) lower than that appeared in ND and SO-supplemented groups.

3.8. Evaluation of the Testis Section

The H&E staining results revealed a loosely arranged tubular structure with inchoate/nebulous spermatocytes and spermatozoa in the testis of ND and SO-supplemented groups (Figure 8A). A higher interstitial gap between the seminiferous tubules was noticed in ND and SO-supplemented groups (Figure 8 A,B and E). While compared to the ND-supplemented group, a significantly 1.4-fold higher ($p<0.001$) interstitial space was observed in the SO-supplemented group, testifying to the adversity of persistent high SO consumption on the testis morphology. Contrary to ND and SO groups, the OSO-supplemented group displayed a compact tubular structure with well-organized/arranged spermatocytes and spermatozoa. In the OSO-supplemented group, a significantly 1.8 ($p<0.001$) and 2.6-fold ($p<0.001$) less interstitial space between the seminiferous tubules was noticed as compared to ND and SO-supplemented groups, respectively (Figure 8 B and E). The results endorsed that OSO had no adverse effect on the testis; instead, it prevented age-associated detrimental effects on the testis.

The DHE fluorescent staining revealed a significantly higher production of ROS in the ND-supplemented group that accounts for 1.3-($p<0.108$) and 1.8-fold ($p<0.01$) higher than the ROS level detected in ND and OSO-supplemented groups (Figure 8 C and F). Consistent with this, approximately 2-fold ($p<0.001$) greater extent of apoptosis was quantified in the ND and OSO supplement group compared to SO and supplemented groups (Figure 8 D and G).

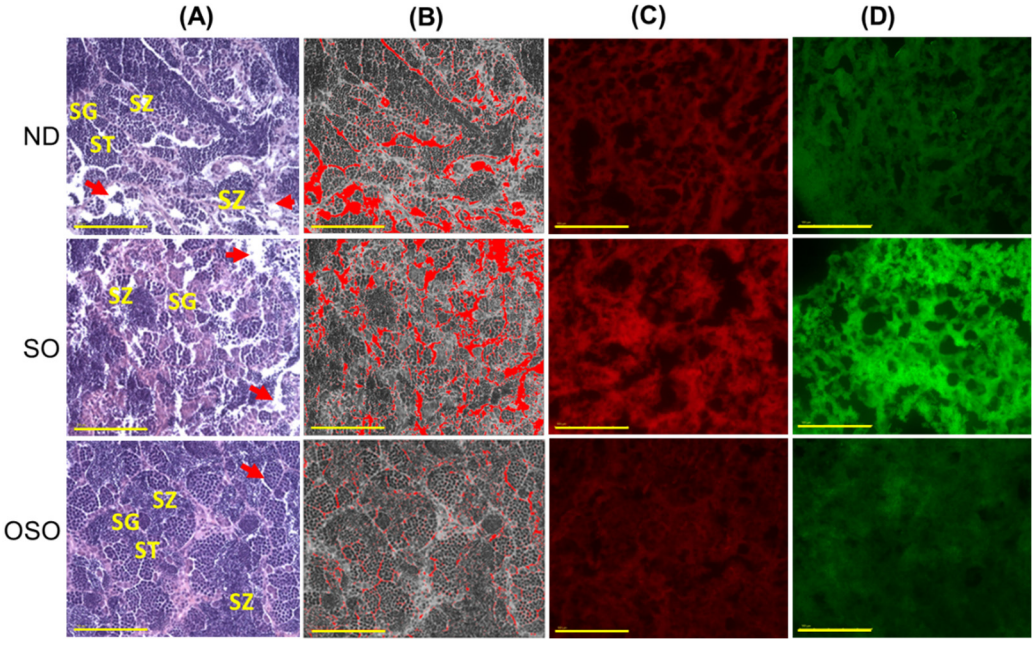

Preprints (www.preprints.org) | NOT PEER-REVIEWED | Posted: 27 November 2023 doi:10.20944/preprints202311.1671.v1

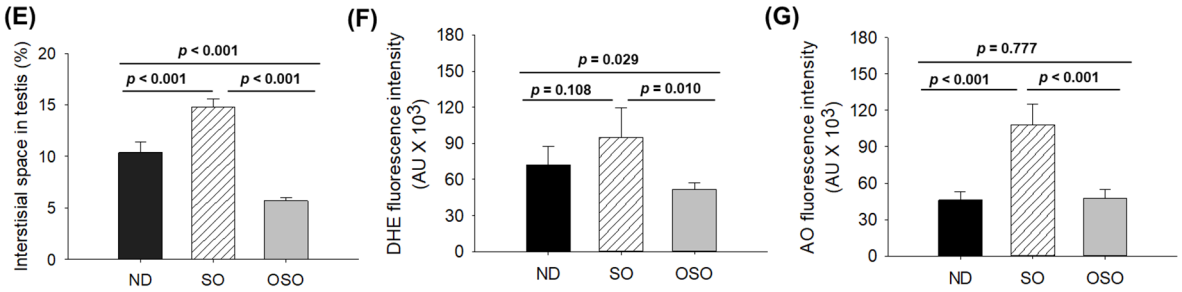

Figure 8. A comparative effect of 24 months of supplementation of sunflower oil (SO) and ozonated sunflower oil (OSO) on the zebrafish testis. **(A)** Testis histology was analyzed by Hematoxylin and eosin (H&E) staining. SG, ST, and SZ represent spermatogenia, spermatocytes and spermatozoa. The red arrow specifies the interstitial space between seminiferous tubules **(B)** Transformation of the white color (void space) that appeared in the H&E section to the red color for the clear visualization of interstitial space between seminiferous tubules (at the threshold value of 220-255) employing Image J software (http://rsb.info.nih.gov/ij/ assessed on 2023 Jan 30). **(C)** and **(D)** DHE and AO-stained area, respectively. [0.1 mm, scale bar]. **(E)** Image J-based quantification of interstitial space in testis. **(F)** and **(G)** Quantification of dihydroethidium (DHE) and acridine orange (AO) fluorescent stained area, respectively, utilizing Image J software. ND represents the control normal diet; SO represents ND supplemented with 20% SO (*wt*/*wt*); OSO represents ND supplemented with 20% OSO (*wt*/*wt*). The *p* value signifies the statistical significance discerned between groups resulting from the one-way ANOVA following Tukey's Post Hoc analysis.

3.9. Plasma Lipid Profile

As depicted in Figure 9, the least amount of TC was observed in the OSO-supplemented group, i.e., significantly 12% (p<0.001) and 14% (p<0.001) lower than the TC level quantified in the ND and SO-supplemented groups, respectively. Interestingly, no significant change in the HDL-C level was noticed in ND, SO, and OSO-supplemented groups. Contrary to this, the HDL/TC level was 32% and 34% higher in OSO-supplemented groups than in ND and SO-supplemented groups. The HDL/TC in the ND and OSO groups quantified nearly the same. The minimum TC level was observed in OSO, i.e., significantly 12% (p<0.001) and 14% (p<0.001) lower than the TC levels of ND and SO-supplemented groups. While compared to SO, the ND group showed a 12% reduced level of TG. Likewise, the lowest level of LDL-C was detected in OSO, which is 12% (p<0.001) and 13% (p<0.001) lower than that of the ND and SO groups, respectively. A nearly similar amount of LDL-C was detected in ND and SO groups. The TG/HDL-C level was significantly 13% (p<0.001) lower in the OSO group compared to the SO group. While compared to ND and SO, a non-significant level of TG/HDL-C was observed. A combined outcome suggests no adverse effect of prolonged OSO supplementation on the lipid profile; infant OSO was observed to exert a positive effect on blood lipid management altered by age-related stress.

Preprints (www.preprints.org) | NOT PEER-REVIEWED | Posted: 27 November 2023 doi:10.20944/preprints202311.1671.v1

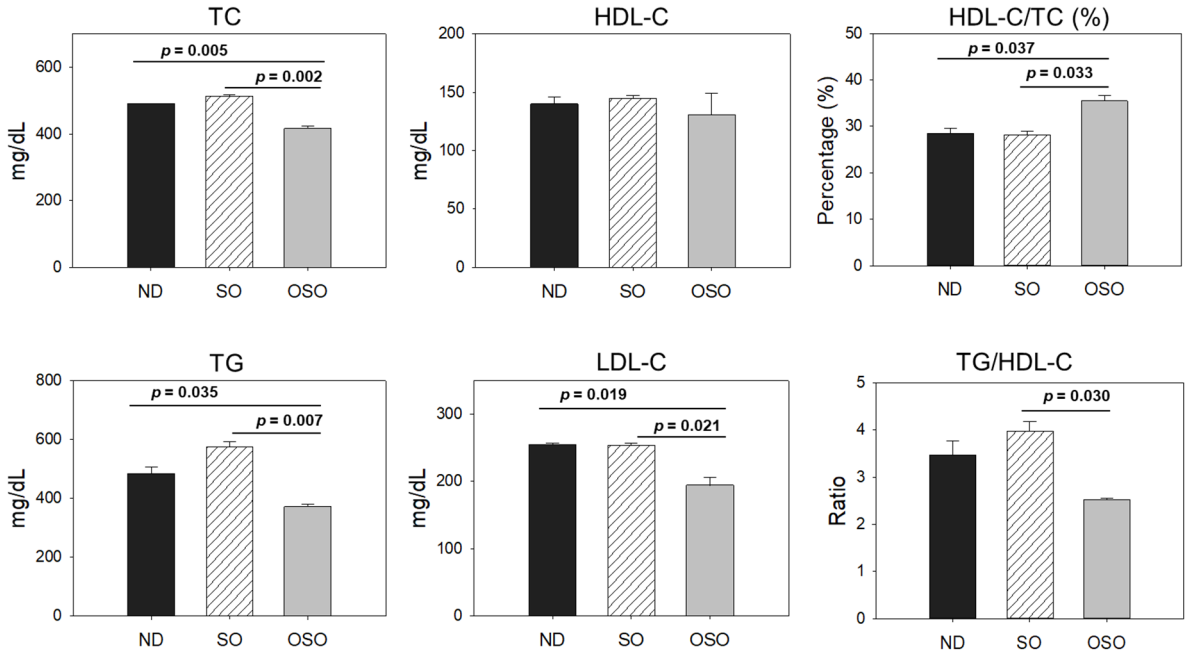

Figure 9. Blood lipid profile of zebrafish fed with sunflower oil (SO) and ozonated sunflower oil (OSO) for 24 months. TC (total cholesterol), TG (triglycerides), HDL-C (high-density lipoprotein cholesterol) and LDL-C (low-density lipoprotein cholesterol), ND represents the control normal diet; SO represents ND supplemented with 20% SO (*wt*/*wt*); OSO represents ND supplemented with 20% OSO (*wt*/*wt*). The *p* value signifies the statistical significance discerned between groups resulting from the one-way ANOVA following Tukey's Post Hoc analysis.

4. Discussion

Ozonated oils are made by pumping the ozone in the oil, where the ozone reacts with the unsaturated side of the fatty acids [8], rendering the functionality of oil. Numerous studies have defined the varied therapeutic potential of ozone [27,28]. In our recent studies, we observed OSO as antimicrobial [9], antioxidant, anti-inflammatory [10,11], and wound healing activity [11]. Extending our earlier finding herein, we have evaluated the impact of prolonged (2 years) consumption of OSO on zebrafish survivability, body weight, liver, kidney, testis, ovary, and age-associated parameters to ascertain whether OSO is toxic or non-toxic when included in the diet. Results outlined the positive effect of OSO on the survivability of zebrafish; contrary to this, the prolonged consumption of SO showed a negative impact on the survivability of zebrafish. Similarly, the consumption of OSO has an anti-obesity effect and maintains the body weight. The study unequivocally established that the existence of ozone-catalyzed compounds in OSO affects zebrafish longevity and body weight management, which are in accordance with the earlier reports highlighting the imperative role of OSO in preventing high cholesterol diet (HCD) induced mortality and body weight maintenance [10].

The average age of zebrafish is approximately 3 years [29], and spinal deformities are a typical age-associated feature of zebrafish [29,30] and thus serve as an indirect marker of aging. The OSO consumption was found to prevent spinal curvature, thus suggesting the anti-aging effect, which strengthen the previous findings of the zebrafish survivability results. The swimming patterns of zebrafish are intricately linked to their muscle mass, which tends to decline with age [31]. Consequently, the abnormalities in muscle mass induced by aging explicitly affect swimming activity. The OSO displayed much better swimming activity than the ND and SO-supplemented groups, indirectly suggesting better muscle mass and less muscle abnormalities. The swimming activity outcome supports the spinal bending results, which are plausibly linked with muscular deformities [29,30]. A combined output of zebrafish survivability, spinal deformities, and swimming behavior strengthens the notion that the OSO can prevent/delay age-associated detrimental effects.

 doi:10.20944/preprints202311.1671.v1

Furthermore, the effect of OSO consumption on the liver was evaluated. The finding concludes the non-hepatotoxic effect of OSO; even more, the OSO displayed a hepatoprotective effect against age-associated stress, evident by a low H&E-stained area. During age, an elevated level of ROS and a compromised antioxidant system leads to oxidative stress, considered the major contributor to age-associated detrimental effects on different organs [32]. We observed that OSO consumption efficiently prevents ROS generation, signifying OSO's antioxidant effect. Mitochondria is the primary source of inheritance ROS generation and is a key contributor to age-related apoptosis [33]. Concurrently, the aging process is associated with endoplasmic reticulum (ER) stress, affecting lipid metabolism, and resulting in apoptosis and the onset of fatty liver disease [34]. Therefore, an antioxidant that efficiently scavenges ROS has a healing effect against oxidative stress indued apoptosis and fatty liver changes. We observed a diminished ROS level, reduced apoptosis, and fatty liver changes in the OSO-supplemented groups, strengthening the notion that the antioxidant nature of OSO is a putative mechanism of hepatoprotection against age-induced adversity. The results aligned well with our previous findings suggesting the antioxidant nature of OSO to prevent the ROS induced apoptotic cell death of mouse brain microglial (BV-2) cells [9]. Consistent with this OSO antioxidant nature rescued zebrafish embryos from apoptotic cell death and teratogenic effects exerted by carboxymethyllysine (CML) an important end glycation ed product (AGEs) [10].

Distinctively, age-associated caspase 3 mediated apoptosis is critical for skeletal muscle atrophy [35] and muscle abnormalities that subsequently impact the zebrafish spinal integrity and swimming behavior. Our earlier results showed a preventive impact of OSO against spinal deformities and swimming activities, strengthening the notion that OSO, owing to its antioxidant and antiapoptotic role, prevents muscular integrity and consequently preserves the spinal deformities and swimming behavior of zebrafish.

Cytokines-mediated inflammation is often observed in the liver with age [33]. There is strong evidence of the age-related elevation of IL-6 [36]; in one such study, a 2.5-fold higher IL-6 production was detected in humans of 85 years and older compared to the human subjects of the 60s and 70s [37]. In the present study, we observed an age-associated elevated IL-6 level in the hepatic tissue of the zebrafish. Nonetheless, the consumption of OSO exhibited a potent anti-inflammatory effect against age-associated IL-6 production. Due to its antioxidant properties, the OSO effectively scavenges ROS, thereby reducing the production of IL-6. The notion is strongly supported by earlier studies suggesting the profound impact of oxidative stress on the induction of inflammation and inflammation-related disorders [38-40]. Contrary to OSO, the SO displayed a higher production of ROS, thus having a higher level of IL-6. The findings align closely with the previous findings, deciphering the OSO antioxidant properties as a critical contributor to inhibiting CML-induced IL-6 levels in the liver of zebrafish [10]. The results demonstrated that the presence of ozone-catalyzed compounds in OSO improves the bio functionality of SO to deal with age-associated stress.

Mounting evidence proves the accumulation of senescent cells with aging; thus, cellular senescence is considered an important biomarker of aging [41]. In the present work, the least cell senescence was observed in the OSO-supplemented group; in contrast, a high prevalence of senescence was observed in the SO-supplemented group. Several intrinsic and extrinsic factors contribute to senescence, and oxidative stress is one of the leading causes of the induction of premature senescence [41]. We assert that the OSO antioxidant properties hinder the generation of ROS, thereby preventing oxidative stress and subsequently inhibiting the senescence process. The senescence in the hepatocyte is also associated with hepatic fat accumulation, cytokine secretion, and proinflammatory factors, leading to fatty liver disease and steatosis [42,43]. Therefore, inhibition in cellular senescence emerges with preventing fatty liver changes. The observed increase in proinflammatory IL-6 expression in the SO-supplemented group is correlated with significant fatty liver changes, possibly attributed to elevated hepatic senescence. Contrary to this, OSO diminishes hepatic senescence owing to its antioxidant nature, thus preventing fatty liver changes and the production of proinflammatory IL-6. In general, all the findings of the hepatic function confirm the hepatoprotective role of OSO by inhibiting age-associated oxidative stress that consequently diminishes the IL-6 production, fatty liver changes, and hepatocyte senescent.

 doi:10.20944/preprints202311.1671.v1

In line with the hepatic tissue analysis, there were no signs of nephrotoxicity following extended OSO supplementation. Contrary to this, a minor histological change was observed in the ND-supplemented group, signifying the impact of aging on the kidney. Aging is a critical intergenic factor that elevates oxidative stress in the kidney [35,44]; consistent with the notion, we also noticed elevated oxidative stress (measured by ROS quantification) in the kidney of the ND-supplemented zebrafish. The prolonged supplementation of SO was observed to augment the age-associated ROS level. In contrast, OSO supplementation displayed a reduced ROS level, which was significantly better than the ND-supplemented group, signifying the importance of ozone-catalyzed compounds to maintain age-altered oxidative stress in the kidney. Also, aging significantly contributes to apoptosis in the kidney via caspase 3 activation, leading to kidney function impairment [35,45]. Therefore, a substance that halts excessive apoptosis in the kidney improves kidney function. The OSO showed a much lower extent of apoptosis than the ND group, suggesting the positive impact of OSO supplementation on preserving kidney functionality against age. As oxidative stress is the primary culprit in inducing the apoptosis and cell senescence following different detrimental effects [46], the antioxidant nature of OSO, evidenced by present findings and documented in the previous reports [9,10], seems to be a key contributor against age-induced apoptosis and cellular senescence in the kidney.

Oxidative stress, inflammation, and apoptosis typically manifest in the aged testis [47], and these factors substantially influence both the quality and quantity of sperm along with the process of spermatogenesis [47]. Therefore, inhibition of apoptosis and oxidative stress in testis leads to preventive events against age-associated impairment. OSO-guided ROS and apoptosis inhibition is the major reason for the age-associated deterioration of testis.

Increasing age significantly affects the functionality and metabolic disorders in ovaries [48]. In the aged ovaries, a high prevalence of sphingomyelin is observed, which leads to critical events in apoptosis [48]. Also, a decreased antioxidant status (reduced glutathione peroxidase and superoxide dismutase levels) was noticed in the aged ovaries that are believed to elicit oxidative stress [48], leading to ovarian dysfunction [49]. The high level of oxidative stress can lead to telomere damage and mitochondrial dysfunction [49] that can lead to cellular senescence in the aged ovaries [50,51]. Therefore, a substance that can counter oxidative stress, apoptosis, and inflammation can induce preventive cellular events against age-associated ovarian damage. We posit that OSO, by virtue of its antioxidant and anti-inflammatory functions, safeguards the ovaries against the adverse impacts of aging. These findings aligned well with the previous reports documenting the impact of varied substances to prevent ovary functionality due to their antioxidant [48,49,52,53] and anti-inflammatory role [51-53].

Accumulating literature suggested the adverse effect of aging on the blood lipid profile [54] that significantly contributes to the onset of cardiovascular diseases [54]. In general, the enhancement of blood TC and LDL-C with the reduction of the HDL-C level are the prominent features of old age [55]. The exact mechanism of age-allied hypercholesteremia has yet to be well understood. However, among the several reasons fatty acids induced insulin resistance, growth hormone deficiency, a decrease of peroxisome proliferator associated receptor α, and liver dysfunction have a notable impact on age-related dyslipidemia [55]. The importance of proinflammatory cytokines like IL-6 has been documented to alter the blood lipid profile [56], signifying the importance of inflammation in dyslipidemia. In the present work, we have observed the reduced level of serum TC, TG, and HDL-C in the OSO-supplemented group along with an alleviated level of IL-6 in the hepatic tissue, which might be a reason for the low lipid level in the OSO-supplemented zebrafish. This notion is firmly substantiated by previous reports revealing a distinct link between inflammatory disorders and the blood lipid profile [57]. We postulated that the anti-inflammatory effect exerted by OSO (suggested by IHC staining) is a pivotal event in maintaining the blood lipid profile in the OSO supplementation zebrafish.

Preprints (www.preprints.org) | NOT PEER-REVIEWED | Posted: 27 November 2023 doi:10.20944/preprints202311.1671.v1

5. Conclusions

A two year OSO consumption displays a non-toxic effect against zebrafish survivability and functionality of vital organs. Moreover, OSO consumption was logged for the preventive effect against age-associated spinal deformities, senescence, and the function of vital organs that found significantly better than the consumption of SO, suggesting the importance of ozone-catalyzed compounds to improve the functionality of SO. The antioxidant and anti-inflammatory nature of OSO was a key regulator responsible for the beneficial effects against age associated adversity of spinal bending, swimming activity, and dyslipidemia (Figure 10). The results endorse OSO's safe and non-toxic nature and propose it as a nutraceutical to prevent age-associated deterioration.

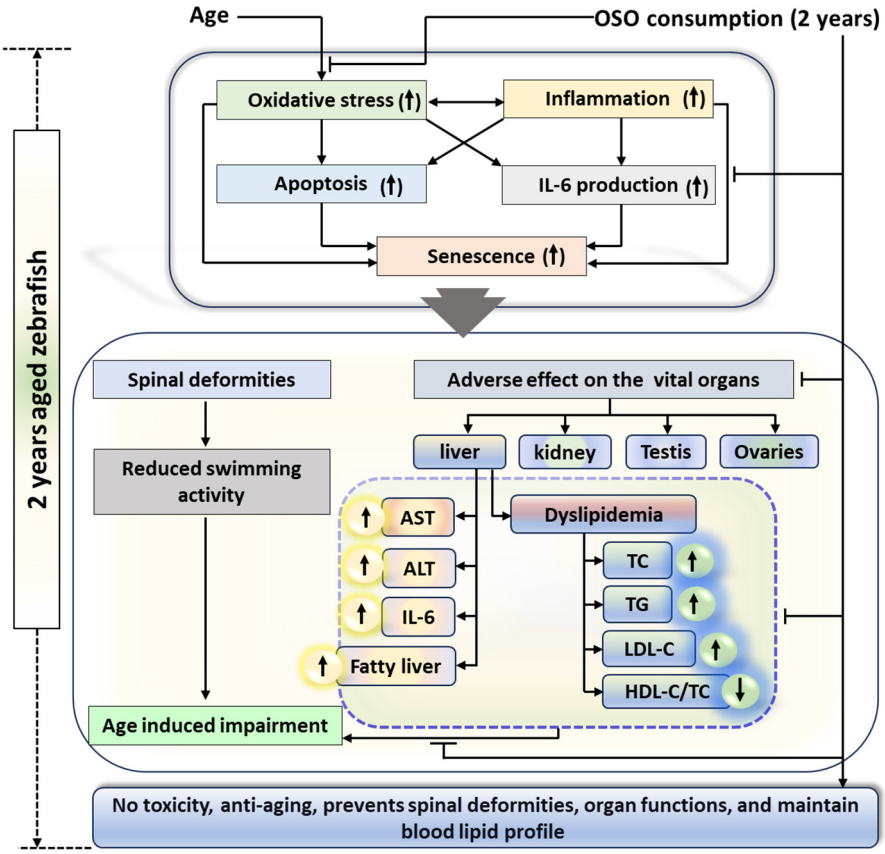

Figure 10. Impact of ozonated sunflower oil (OSO) consumption for 2 years on the age associated changes in zebrafish.

Supplementary Materials: Supplementary video 1: Swimming behavior of zebrafish after 28 months supplementation of normal diet (ND), sunflower oil (SO) and ozonated sunflower oil (OSO).

Author Contributions: Conceptualization, K.-H.C.; methodology, J.-E.K., D.-J.K. and A.B.; data curation, writing—original draft preparation, K.-H.C.; writing—review and editing, K.-H.C., supervision, K.-H.C.; All authors have read and agreed to the published version of the manuscript.

Funding: This research received no external funding.

Institutional Review Board Statement: The animal study protocol was approved by Committee of Animal Care and Use of Raydel Research Institute (approval code RRI-20-004).

Informed Consent Statement: Not applicable.

Data Availability Statement: The data used to support the findings of this study are available from the corresponding author upon reasonable request.

Conflicts of Interest: The authors declare no conflict of interest.

References

1. Skorić, D.; Jocić, S.; Sakac, Z.; Lecić, N. Genetic possibilities for altering sunflower oil quality to obtain novel oils. *Can. J. Physiol. Pharmacol.* **2008,** *86*, 215–221.
2. Adeleke, B.S.; Babalola, O.O. Oilseed crop sunflower (*Helianthus annuus*) as a source of food: Nutritional and health benefits. *Food Sci. Nutr.* **2020**, *8*, 4666–4684.
3. Raß, M.; Schein, C.; Matthäus, B. Virgin sunflower oil. *Eur. J. Lipid Sci. Technol.* **2008**, *110*, 618–624.
4. Khan, S.; Choudhary, S.; Pandey, A.; Khan, M.K.; Thomas, G. Sunflower oil: Efficient oil source for human consumption. *Emergent Life Sci. Res.* **2015**, *1*, 1–3.
5. Tokur, B.; Korkmaz, K.; Uçar, Y. Enhancing sunflower oil by the addition of commercial thyme and rosemary essential oils: The effect on lipid quality of Mediterranean horse mackerel and anchovy during traditional pan-frying. *Int. J. Gastron. Food Sci.* **2021**, *26*, 100428.
6. Díaz, M.F.; Sánchez, Y.; Gómez, M.; Hernández, F.; Da, C.; Veloso, M.C.; De, P.; Pereira, P.A.; Mangrich, A.S.; De Andrade, J.B. Physicochemical characteristics of ozonated sunflower oils obtained by different procedures. *Grasas Y Aceites* **2012**, *63*, 466–474.
7. Preuss, F. Ozone oxidation of fatty acid thin films: a TIR Raman study. 2022. https://www.diva-portal.org/smash/record.jsf?pid=diva2:1701750
8. Ugazio, E.; Tullio, V.; Binello, A.; Tagliapietra, S.; Dosio, F. Ozonated oils as antimicrobial systems in topical applications. Their characterization, current applications, and advances in improved delivery techniques. *Molecules* **2020**, *25*, 334.
9. Cho, K.-H.; Kang, D.-J.; Nam, H.-S.; Kim, J.-H.; Kim, S.-Y.; Lee, J.-O.; Kim, B.-J. Ozonated sunflower oil exerted protective effect for embryo and cell survival via potent reduction power and antioxidant activity in HDL with strong antimicrobial activity. *Antioxidants* **2021**, *10*, 1651.
10. Cho, K.-H.; Kim, J.-E.; Bahuguna, A.; Kang, D.-J. Long-term supplementation of ozonated sunflower oil improves dyslipidemia and hepatic inflammation in hyperlipidemic zebrafish: Suppression of oxidative stress and inflammation against carboxymethyllysine toxicity. *Antioxidants* **2023**, *12*, 1240.
11. Cho, K.-H.; Kim, J.-E.; Bahuguna, A.; Kang, D.-J. Ozonated sunflower oil exerted potent anti-inflammatory activities with enhanced wound healing and tissue regeneration abilities against acute toxicity of carboxymethyllysine in zebrafish with improved blood lipid profile. *Antioxidants* **2023**, *12*, 1625.
12. Ginel, P.J.; Negrini, J.; Guerra, R.; Lucena, R.; Ruiz-Campillo, M.T.; Mozos, E. Effect of topical ozonated sunflower oil on second intention wound healing in turtles: a randomised experimental study. *J. Vet. Sci.* **2021**, *22*, e27.
13. Zamora Rodríguez, Z.B.; González Alvarez, R.; Guanche, D.; Merino, N.; Hernández Rosales, F.; Menéndez Cepero, S.; Alonso González, Y.; Schulz, S. Antioxidant mechanism is involved in the gastroprotective effects of ozonized sunflower oil in ethanol-induced ulcers in rats. *Mediat. Inflamm.* **2007**, *2007*, 65873.
14. Zeng, J.; Lu, J. Mechanisms of action involved in ozone-therapy in skin diseases. *Int. Immunopharmacol.* **2018**, *56*, 235–241.
15. Ozturk, B.; Kurtoglu, T.; Durmaz, S.; Kozaci, L.D.; Abacigil, F.; Ertugrul, B.; Erel, O. The effects of ozone on bacterial growth and thiol-disulphide homeostasis in vascular graft infection caused by MRSA in rats. *Acta Cir. Bras.* **2017**, *32*, 219–228.
16. Jenerowicz, D.; Silny, W.; Da´nczak-Pazdrowska, A.; Pola´nska, A.; Osmola-Ma´nkowska, A.; Olek-Hrab, K. Environmental factors and allergic diseases. *Ann. Agric. Environ. Med.* **2012**, *19*, 475–481.
17. Borges, G.Á.; Elias, S.T.; da Silva, S.M.M.; Magalhães, P.O.; Macedo, S.B.; Ribeiro, A.P.D.; Guerra, E.N.S. In vitro evaluation of wound healing and antimicrobial potential of ozone therapy. *J. Cranio-Maxillofac. Surg.* **2017**, *45*, 364–370.
18. Menéndez, S.; Falcón, L.; Maqueira, Y. Therapeutic efficacy of topical OLEOZON® in patients suffering from onychomycosis. *Mycoses* **2011**, *54*, 272–277.
19. Nusslein-Volhard, C.; Dahm, R. Zebrafish: A practical approach, 1st ed.; Oxford University Press: Oxford, UK, 2002.
20. (NRC) National Research Council of the National Academy of Sciences. Guide for the care and use of laboratory animals; national academy press: Washington, DC, USA, 2010.
21. Fischer, A.H.; Jacobson, K.A.; Rose, J.; Zeller, R. Hematoxylin and eosin staining of tissue and cell sections. In *Basic Methods in Microscopy*; Cold Spring Harbor Laboratory Press: New York, NY, USA, 2006; Chapter 4.

22. Cho, K.-H.; Nam, H.-S.; Kim, J.-E.; Na, H.-J.; del Carmen Dominguez-Horta, M.; Martinez-Donato, G. CIGB-258 exerts potent anti-inflammatory activity against carboxymethyllysine-induced acute inflammation in hyperlipidemic zebrafish via the protection of apolipoprotein AI. *Int. J. Mol. Sci.* **2023,** *24*, 7044.
23. Hull, L.C.; Sen, R.; Menzel, J.; Goyama, S.; Kurokawa, M.; Artinger, K.B. The conserved and divergent roles of Prdm3 and Prdm16 in zebrafish and mouse craniofacial development. *Dev. Biol.* **2020**, *461*, 132–144.
24. Owusu-Ansah, E.; Yavari, A.; Mandal, S.; Banerjee, U. Distinct mitochondrial retrograde signals control the G1-S cell cycle checkpoint. *Nat. Genet.* **2008**, *40*, 356–361.
25. Umali, J.; Hawkey-Noble, A.; French, C.R. Loss of foxc1 in zebrafish reduces optic nerve size and cell number in the retinal ganglion cell layer. *Vision Res.* **2019**, *156*, 66–72.
26. Kim, S.H.; Yadav, D.; Kim, S.J.; Kim, J.R.; Cho, K.-H. High consumption of iron exacerbates hyperlipidemia, atherosclerosis, and female sterility in zebrafish via acceleration of glycation and degradation of serum lipoproteins. *Nutrients* **2017**, *9*, 690.
27. Di Mauro, R.; Cantarella, G.; Bernardini, R.; Di Rosa, M.; Barbagallo, I.; Distefano, A.; Longhitano, L.; Vicario, N.; Nicolosi, D.; Lazzarino, G.; Tibullo, D.; Gulino, M.E.; Spampinato, M.; Avola, R.; Li Volti, G. The biochemical and pharmacological properties of ozone: The smell of protection in acute and chronic diseases. *Int. J. Mol. Sci.* **2019,** *20*, 634.
28. Liu, L.; Zeng, L.; Gao, L.; Zeng, J.; Lu, J. Ozone therapy for skin diseases: Cellular and molecular mechanisms. *Int. Wound J.* **2022,** 1–10.
29. Kishi, S.; Slack, B.E.; Uchiyama, J.; Zhdanova, I.V. Zebrafish as a genetic model in biological and behavioral gerontology: Where development meets aging in vertebrates—A mini-review. *Gerontology* **2009**, *55*, 430–441.
30. Gerhard, G.S.; Kauffman, E.J.; Wang, X.; Stewart, R.; Moore, J.L.; Kasales, C.J.; Demidenko, E.; Cheng, K.C. Life spans and senescent phenotypes in two strains of zebrafish *(Danio rerio)*. *Exp. Gerontol.* **2002**, *37*, 1055–1068.
31. Gilbert, M.J.; Zerulla, T.C.; Tierney, K.B. Zebrafish (*Danio rerio*) as a model for the study of aging and exercise: physical ability and trainability decrease with age. Exp. Gerontol. **2014**, *50*, 106–113.
32. Maldonado, E.; Morales-Pison, S.; Urbina, F.; Solari, A. Aging hallmarks and the role of oxidative stress. *Antioxidants* **2023**, *12*, 651.
33. Hu, S.-J.; Jiang, S.-S.; Zhang, J.; Luo, D.; Yu, B.; Yang, L.-Y.; Zhong, H.; Yang, M.-W.; Liu, L.-Y.; Hong, F.-F.; et al. Effects of apoptosis on liver aging. *World J. Clin. Cases* **2019**, *7*, 691–704.
34. Fu, S.; Watkins, S.M.; Hotamisligil, G.S. The role of endoplasmic reticulum in hepatic lipid homeostasis and stress signaling. *Cell Metab.* **2012**, *15,* 623–634.
35. Tower, J. Programmed cell death in aging. *Ageing res. Rev.* **2015**, *23*, 90–100.
36. Maggio, M.; Guralnik, J.M.; Longo, D.L.; Ferrucci, L. Interleukin-6 in aging and chronic disease: a magnificent pathway. *J. Gerontol. A Biol. Sci. Med. Sci.* **2006**, *61*, 575–584.
37. Ferrucci, L.; Corsi, A.; Lauretani, F.; Bandinelli, S.; Bartali, B.; Taub, D.D.; Guralnik; J.M; Longo, D.L. The origins of age-related proinflammatory state. *Blood* **2005**, *105*, 2294–2299.
38. Sarkar, D.; Fisher, P.B. Molecular mechanisms of aging-associated inflammation. *Cancer Lett.* **2006**, *236*, 13–23.
39. Khansari, N.; Shakiba, Y.; Mahmoudi, M. Chronic inflammation and oxidative stress as a major cause of age-related diseases and cancer. *Recent Pat. Inflamm. Allergy Drug Discov.* **2009**, *3*, 73–80.
40. Zuo, L.; Prather, E.R.; Stetskiv, M.; Garrison, D.E.; Meade, J.R.; Peace, T.I.; Zhou, T. Inflammaging and oxidative stress in human diseases: From molecular mechanisms to novel treatments. *Int. J. Mol. Sci.* **2019**, *20*, 4472.
41. Mohamad Kamal, N.S.; Safuan, S.; Shamsuddin, S.; Foroozandeh, P. Aging of the cells: Insight into cellular senescence and detection methods. *Eur. J. Cell Biol.* **2020**, *99*, 151108.
42. Wiemann, S.U.; Satyanarayana, A.; Tsahuridu, M.; Tillmann, H.L.; Zender, L.; Klempnauer, J.; Flemming, P.; Franco, S.; Blasco, M.A.; Manns, M.P.; et al. Hepatocyte telomere shortening and senescence are general markers of human liver cirrhosis. *FASEB J.* **2002**, *16*, 935–942.
43. Guo, M. Cellular senescence and liver disease: Mechanisms and therapeutic strategies. *Biomed. Pharmacother.* **2017**, *96*, 1527–1537.
44. Gomes, P.; Simão, S.; Silva, E.; Pinto, V.; Amaral, J.S.; Afonso, J.; Serrão, M.P.; Pinho, M.J.; Soares-da-Silva, P. Aging increases oxidative stress and renal expression of oxidant and antioxidant enzymes that are associated with an increased trend in systolic blood pressure. *Oxid. Med. Cell. Longev.* **2009**, *2*, 19–26.

45. Wang, X.; Bonventre, J.V.; Parrish, A.R. The aging kidney: Increased susceptibility to nephrotoxicity. *Int. J. Mol. Sci.* **2014**, *15*, 15358–15376.
46. Pole, A.; Dimri, M.; Dimri, G. Oxidative stress, cellular senescence and ageing. *AIMS Mol. Sci.* **2016**, *3*, 300–324.
47. Matzkin, M.E.; Calandra, R.S.; Rossi, S.P.; Bartke, A.; Frungieri, M.B. Hallmarks of testicular aging: The challenge of anti-inflammatory and antioxidant therapies using natural and/or pharmacological compounds to improve the physiopathological status of the aged male gonad. *Cells* **2021**, *10*, 3114.
48. Li, C.J.; Lin, L.T.; Tsai, H.W.; Chern, C.U.; Wen, Z.H.; Wang, P.H.; Tsui, K.H. The molecular regulation in the pathophysiology in ovarian aging. *Aging Dis.* **2021**, *12*, 934–949.
49. Timóteo-Ferreira, F.; Abreu, D.; Mendes, S.; Matos, L.; Rodrigues, A.R.; Almeida, H.; Silva, E. Redox imbalance in age-related ovarian dysfunction and perspectives for its prevention. *Ageing Res. Rev.* **2021**, *68*, 101345.
50. Kasapoglu, I.; Seli, E. Mitochondrial dysfunction and ovarian aging. *Endocrinology* **2020**, *161*, bqaa001.
51. Kang, M.-H.; Kim, Y.J.; Cho, M.J.; Jang, J.; Koo, Y.D.; Kim, S.H.; Lee, J.H. Mitigating age-related ovarian dysfunction with the anti-inflammatory agent MIT-001. *Int. J. Mol. Sci.* **2023**, *24*, 15158.
52. Nehra, D.; Le, H.D.; Fallon, E.M.; Carlson, S.J.; Woods, D.; White, Y.A.; Pan, A.H.; Guo, L.; Rodig, S.J.; Tilly, J.L.; et al. Prolonging the female reproductive lifespan and improving egg quality with dietary omega-3 fatty acids. *Aging Cell* **2012**, *11*, 1046–1054.
53. Song, C.; Peng, W.; Yin, S.; Zhao, J.; Fu, B.; Zhang, J.; Mao, T.; Wu, H.; Zhang, Y. Melatonin improves age-induced fertility decline and attenuates ovarian mitochondrial oxidative stress in mice. *Sci. Rep.* **2016**, *6*, 35165.
54. Cho, S.M.J.; Lee, H.J.; Shim, J.S.; Song, B.M.; Kim, H.C. Associations between age and dyslipidemia are differed by education level: The cardiovascular and metabolic diseases etiology research center (CMERC) cohort. *Lipids Health Dis.* **2020**, *19*, 12.
55. Liu, H.-H.; Li, J.-J. Aging and dyslipidemia: A review of potential mechanisms. *Ageing Res. Rev.* **2015**, *19*, 43–52
56. Khovidhunkit, W.; Kim, M.S.; Memon, R.A.; Shigenaga, J.K.; Moser, A.H.; Feingold, K.R.; Grunfeld, C. Effects of infection and inflammation on lipid and lipoprotein metabolism: mechanisms and consequences to the host. *J. Lipid Res.* **2004**, *45*, 1169–1196.
57. Feingold, K.R.; Grunfeld, C. The Effect of Inflammation and Infection on Lipids and Lipoproteins. In *Endotext*; De Groot, L.J., Chrousos, G., Dungan, K., Feingold, K.R., Grossman, A., Hershman, J.M., Koch, C., Korbonits, M., McLachlan, R., New, M., et al., Eds.; MDText.com, Inc.: South Dartmouth, MA, USA, 2000.